SCIENTIFIC Publishing Limited

New Energy Exploitation and Application

http://ojs.ukscip.com/index.php/neea

Article

Design and Performance Analysis of Motor Drive System of Light Electric Vehicle

M. Satyendra Kumar Shet [1] **and Shripad T. Revankar** [2,*]

[1] Department of Electrical and Electronics Engineering, NMAM Institute of Technology, Nitte 574110, India

[2] School of Nuclear Engineering, Purdue University, West Lafayette, IN 47907, USA

[*] Correspondence: shripad@purdue.edu

Received: 10 March 2025; **Revised:** 31 March 2025; **Accepted:** 1 April 2025; **Published:** 13 May 2025

Abstract: In this study, the development of vehicle dynamics models and analysis has been carried out for a light electric vehicle (LEV) based on a force model, torque, power-speed profile, the driving cycle, and motor parameters. The proposed customized Electric Propulsion System (EPS) of the LEV consists of a unique 1.5 kW, 3-phase, 4-pole rectangular wave operation Permanent Magnet Brushless DC (PMBLDC) motor with a battery as an energy storage system, which is capable of running at speeds of about 30 km hr^{-1} up to 40 km hr^{-1} with a curb weight of 200 kg. Successfully integrating and optimizing the multidisciplinary subcomponents including Vehicle Body Structure (VBS), Electric Propulsion System (EPS), Energy Storage System (ESS), and Energy Management System (EMS) of the LEV system requires addressing challenges such as weight, safety, reliability, and cost while meeting the demands of diverse driving profiles and operational conditions. A simulation case study for the performance analysis of a 1.5 kW battery-supported motor drive for the LEV has been carried out. Experiments have also been conducted on the performance of the permanent magnet brushless DC (PMBLDC) motor under different load conditions. From the case study, it has been found that the designed customized drive achieves maximum torque density with small torque pulsation through design optimization and a cost-effective Proportional Integral (PI) Control technique. Furthermore, the drive eliminates input distortions and is characterized by low power consumption and high efficiency.

Keywords: Light Electric Vehicles; Design Model; PMBLDC Hub Motor Drive; Vehicle Dynamics; High-Speed Control Accuracy; Experimental Validation

1. Introduction

Concerns on climate change due to pollution from fossil fuel use, specifically in transportation, have led to significant interest in opting for light electric vehicles (LEVs) rather than internal combustion engine vehicles (ICEs). The performance study and analysis are requirements for the desired application. The key requirements of LEVs are reliability, precise accuracy in high-speed control, good dynamic response, noise pollution-free operation, high efficiency with cost-effectiveness, and low maintenance, for which the appropriate choice of electrical machine and drive technology is a key factor. This key factor is known as the powertrain of the LEV, which depends on the performance study and analysis of the Propulsion System (PS) design of the LEV drive. However, it is an intricate process. In this intricate process, the vehicle dynamics-based propulsion system design methodology will serve as a primary foundation to develop a detailed LEV drive. Electric Vehicle Technology (EVT) [1–3] is an integration of subsystems namely the Vehicle Body Structure (VBS), Electric Propulsion System (EPS), Energy Storage System (ESS), and Energy Management System (EMS). Hence, it is an integration of diversified fields of engineering.

Normally LEVs are preferable for short-distance driving at low speeds with a maximum number of stops associated with comfortable charging points within the distance to be travelled. The challenging requirements of light electric vehicles are:

1. Vehicle characteristics: such as size, weight, overload and aerodynamics in order to determine the speed, torque and power required by the motor which are essential for the precise selection of the powertrain.
2. Driving Cycle: i.e., the usage of LEV, in order to determine the configuration of the vehicle and battery size which will impact the choice of the powertrain.
3. Vehicle configuration: i.e., either totally electric or hybrid type.
4. Maximum Speed: i.e., to know the continuous maximum speed of the LEV for a given time duration in order to determine the maximum speed of the motor.
5. Maximum Torque: i.e., required to facilitate the LEV in hill climbing mode with maximum weight.
6. Maximum Power: i.e., required for power to the LEV to reach and maintain a constant speed under stringent slope and speed conditions. In order to calculate the maximum power in addition to the forces needed for the hill climb slope drag and friction coefficients are taken into account. Hence, motor selection for LEV applications should be for the worst hill climb conditions without time limitation.
7. Battery as Energy Source: i.e., required for typical usage of the LEV which can be calculated from the consumption of the vehicle in kWh km^{-1}. The capacity of the energy source or battery can be calculated by multiplying it with the desired range, and the battery voltage is dependent on the size of the vehicle and, finally, the cost of the LEV. Selection of electric motor for electric vehicle application depends upon these above-mentioned points in addition to with or without gearbox and the cost [4].

The selection of the electric motor for electric vehicle applications depends on the above-mentioned points, in addition to whether it has a gearbox and the cost. Hence, suitable integration and coordination of all the components of this system is of utmost importance to address issues like weight, volume, driving profile, transport operating and temperature conditions, safety, reliability, and cost economics. To propel the vehicle and to overcome the aerodynamic drag, rolling resistance drag and kinetic resistance, the EPS system is required. This system converts electrical power into mechanical power. The schematic diagram of the EPS is shown in **Figure 1**. This system primarily consists of a motor, converter, controller unit, and energy storage, among which the motor is considered the "heart" of the EPS applicable to EV.

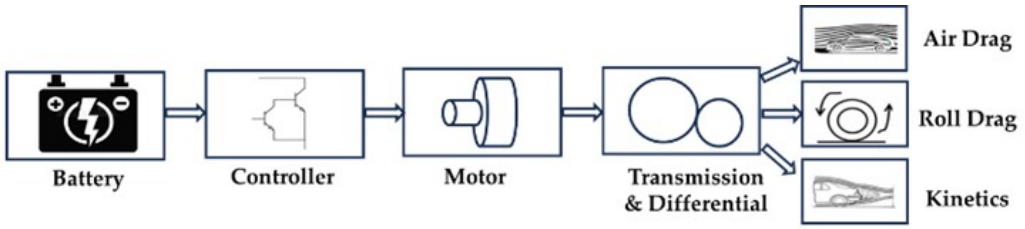

Figure 1. Battery electric propulsion system.

Hence, a major challenging area in the suitable configuration of the Electrical Propulsion System (EPS) is the design, development of the model, analysis, simulations studies and finally possible real-time implementations of a viable motor-based drive system. The appropriate size and integration of various components of EPS is really an overall challenging task including the cost [5–7]. Therefore, the key factor of the EV drive system is the suitable choice of motor and drive technology.

The vehicle operation consists of three main sectors: namely: the starting acceleration, cruising at vehicle rated speed, and cruising at the maximum speed with minimum power. These three LEV operations provide the fundamental design constraints for the drive train of the LEV. For viable real-time product manufacturing, the refinement of these basic design constraints is necessary, which is beyond the scope of this paper. The main aim at present is to overcome these design constraints with minimum power [8]. Classification of BLDC Motors is shown in **Figure 2** [9]. Comparative performance parameters, in terms of grading from 1 to 10 points for a few of these

motors, are also shown in **Table 1**, in which 1 is the worst and 10 is the best. Technical features of PMBLDC motors in comparison to other motors, as mentioned in **Table 2**, show that they are best suited for LEV applications [10]. Also, the efficiency of Permanent Magnet motors is also higher than that of other motors (greater than 90%) [11–14].

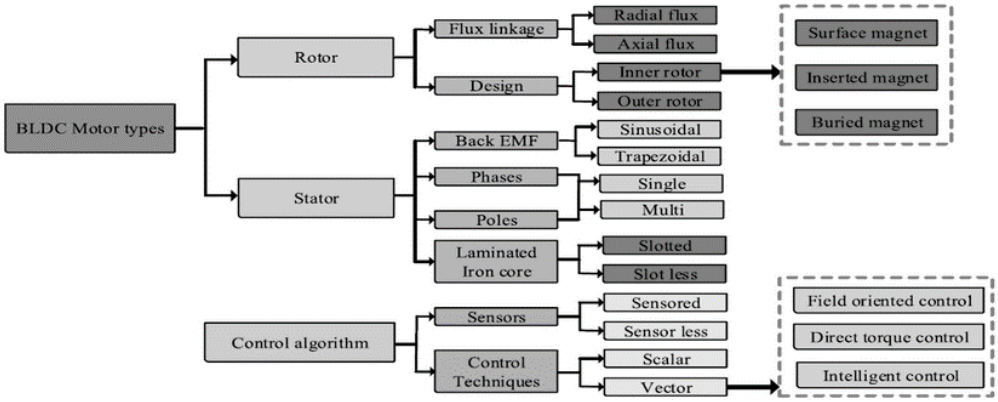

Figure 2. LEV motor classification [9].

Table 1. Parameter comparison of EV motors.

Sl.No.	Parameters	IM	PMBLDC	PMH	SRM
1.	Torque-speed characteristics	10	10	10	10
2.	Power density	05	10	08	06
3.	Robustness	08	08	08	10
4.	Thermal management	08	10	08	10
5.	Status	10	08	06	06
	Total	47	54	50	48

The drive technology consists of power electronic converters of different topologies namely inverter, dc-dc converter, and rectifier, with devices like MOSFET, IGBT, and SiC devices, along with control units of hardware and software, namely microprocessor (μp), microcontroller (μc), Digital Signal Processing(DSP), Field Programmable Gate Array (FPGA), dSPACE, V/F control, Field Oriented Control (FOC), Direct Torque Control (DTC), Genetic Algorithm (GA), Artificial Neural Network (ANN) work, Fuzzy Logic (FL), and Artificial Intelligence (AI), etc.

The motor to be used for the light electric vehicle drive cannot be compared with standard industrial application motors. The appropriate choice of electric vehicle motor depends on torque/speed characteristics. **Figure 3a** shows the motor torque/speed characteristics for LEV applications [15], and **Figure 3b** shows motor torque/speed characteristics general for industrial purposes [3, 16]. The choice of electric motor is an important feature in the overall Electric Propulsion System (EPS) design.

Table 2. Comparison of technical features of types of motors [17, 18].

Sl.No.	Parameters	IM	PMBLDC	DCM
1.	Torque-speed characteristics	Non-linear	Linear	Fairly plane
2.	Starting current	5–7 times rated current	Rated current	Twice the rated current
3.	Motor rating	Reasonable/Low	High	Low
4.	Efficiency	Low	High	Moderate
5.	Control	Simple and cheaper	Complex and costly	Simple and cheaper
6.	Commutation	Not applicable	Electronic	Brushed
7.	Speed range	High	High	Low
8.	Slip	Present	NA	NA
9.	Noise	Moderate	Low	High
10.	Maintenance and durability	Regular and high	Less and modest	Regular and low

The architecture of the LEV is shown in **Figure 4** [19], in which the motor is powered by the batteries through the electronic controllers. The controller receives the signal for the estimated power to be given for the intended load situation from zero to full power through the accelerator knob connected to a pair of potentiometers or variable resistors [6, 20]. The in-wheel hub motor EV drive system is preferable for LEVs because the wheel can be easily fixed over the hub rotor or outer rotor-based configuration and technology of the PMBLDC motor.

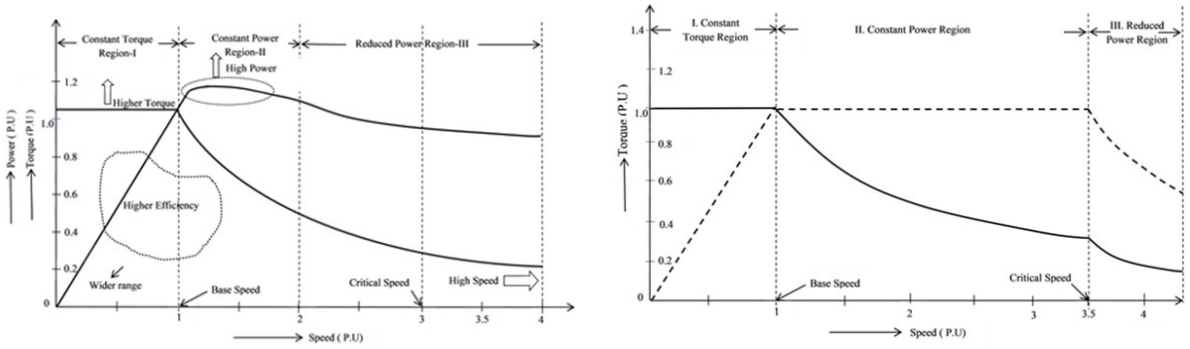

(**a**) (**b**)

Figure 3. (**a**) LEV application torque-speed characteristics, and (**b**) General industrial application torque-speed characteristics.

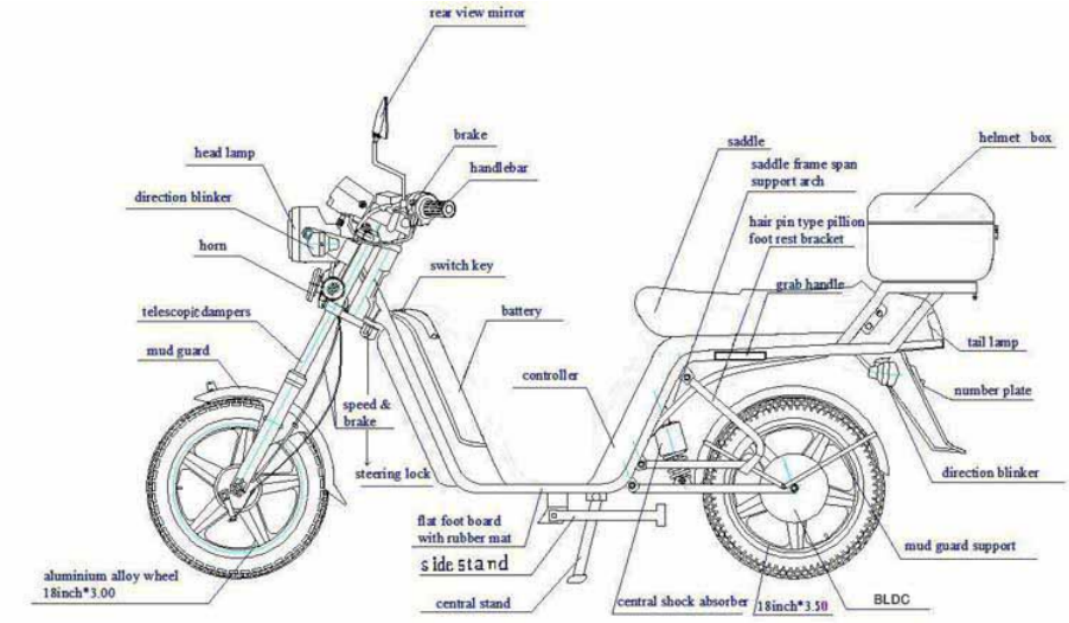

Figure 4. Architecture of LEV-typical battery electric scooter.

The objective of this paper is to investigate and analyze the vehicle dynamics-based propulsion system design in order to meet the vehicle operational constraints with minimum power requirements, aiming to arrive the minimum LEV drive weight, volume, and cost-effectiveness. Additionally, the torque produced by the motor of the EPS must overcome aerodynamic drag and the tractive force of the load i.e., the road and driving conditions. This study provides insight into the viability of developing such a transport system to find its suitability for the application of Indian coastal topographical roads, which consists of a combination of ascending altitude, descending altitude and horizontal drive. In this study, the customized EPS of the LEV consists of a 1.5 kW motor with a battery as an energy storage system, capable of ascending altitude without increasing the motor rated power and battery capacity, and is

also capable of running at speeds of about 30 km hr–1 up to 40 km hr–1 to suit Indian coastal topographical driving conditions.

The case study focuses on (1) vehicle dynamics, and (2) a design methodology based on the three regions of operation (3) drive cycle analysis to choose power rating of the motor and suitable choice of motor, (4) simulation case studies of the PS design of the LEV drive for the same vehicle parameters chosen, and (5) validation of the same by prototype and experimental results. The PS design is developed for a weight of 200 kg, at speeds of 30 km h^{-1} to 40 km h^{-1} and an approximate altitude of 15° to 20°, suitable for both urban and rural driving by incorporating a 1.5 kW PMBLDC hub motor. The presented simulation case study results of the segments of the propulsion system design for the same vehicle parameters chosen are in line and found suitable for the desired LEV drive. Certainly, in today's context, the two-wheeler transportation system has become a need of the society in both urban and rural areas. This paper presents the LEV propulsion system design philosophies.

The paper is organized as follows: Section 2 provides details related to the design and development of the dynamic force model applicable to LEVs. This is required to calculate the essential power of the LEV drive. The forces acting on the vehicle are assessed and the average power needed to drive the vehicle has been calculated. Further, the simulation case study to analyze both force-speed and power-speed profiles has been carried out and presented for the chosen vehicle parameters. Section 3 deals with the drive cycle, in which a comparative study is carried out by considering both the New European Driving Cycle (NEDC) and the Indian Driving Cycle (IDC) for the same duration of 1200 seconds. The relationship of the torque and speed to the tire diameter has been illustrated and explained in detail with the aid of a simulation case study of the force model and driving profile for the same vehicle parameters. From the comparative study analysis of NEDC and IDC, the torque and power profile has been developed to calculate the required motor power rating, which is 1.5 kW in this case study. In Section 4, the performance analysis of the LEV drive for rated speed and at different drive conditions has been evaluated for the same vehicle parameters chosen in Sections 2 and 3. Further, in this section, it is validated that the selected motor design parameters and specifications exactly matche the vehicle parameters of Section 2. The performance characteristics such as output power, output torque, efficiency and input DC current have been obtained. From the presented case study simulation results, it is observed that the efficiency is high, at about 90% for approximately 1430 rpm, and the maximum output power is about 48.52 kW at 715 rpm, reaching zero at 1500 rpm. Also, the starting high input motor current yields a considerable magnetic saturation level of the stator during which the motor speed is much lower, and as this motor speed increases, the input motor current starts decreasing and reaches zero at 1500 rpm. The motor rated torque generated is 14.23 Nm without saturation. In Section 5, the experimental implementation of the propulsion system design with results has been presented. The EPS optimized output is obtained at different driving conditions. The uniqueness of this work is the investigation and analysis of the vehicle dynamics, which provides insight into the viability of developing such a transport system to find its suitability for the application of Indian coastal topographical roads.

2. Design of Dynamic Electric Force Model of LEV Drive

The vital design considerations of LEVs are: torque developed by the motor, power, speed and size of the motor, and capability of the desired recharging driving range. The electric propulsion system of the LEV is responsible for converting electrical energy to mechanical energy in such a way that the vehicle is propelled to overcome aerodynamic drag, rolling resistance drag and kinetic resistance. Hence, the first step in performance modeling of the electric scooter is to derive the electric force model, which is essential for the appropriate choice of motor [21]. This electric force, through the drive wheels, will pass on to the ground, thereby propelling the electric scooter in a forward direction. This electric force should overcome the loading of the road and accelerate the scooter. Therefore, the designed motor should offer adequate force to overcome: (1) aerodynamic drag, (2) rolling resistance force and (3) the weight of the scooter acting on the incline, allowing the scooter to accelerate.

The specifications of the LEV propulsion system design are: (1) design constraints, (2) design variables and (3) road load characteristics.

2.1. Design Constraints

The vehicle operation consists of three main sectors: namely, the starting acceleration, cruising at vehicle rated speed, and cruising at the maximum speed with minimum power. These three LEV operations provide the fundamental design limitations for the drive train of the vehicle. The main objective of the LEV propulsion system design is to overcome the vehicle operation constraints: namely: (1) the initial acceleration, (2) cruising at vehicle rated speed, and (3) cruising at the maximum speed with minimum power. The variable parameters of this propulsion system design constraint are: (1) rated velocity (v_{rv}) of the LEV, (2) specified time (t_s) to reach the defined rated velocity of the LEV, (3) maximum velocity(v_{max}) of the LEV, and (4) mass and other body dimensions of the LEV.

2.2. Design Variables

The powertrain is the key component of LEV. The variables of the propulsion system designs are: (1) rated motor power (P_m), (2) rated motor speed (v_{rm}), (3) maximum speed of the motor, (4) wide-range constant power region operation beyond the rated speed, and (5) the gear ratio between the shaft of the motor and the wheel. As stated above, the main objective of the LEV propulsion system design is to ascertain the minimum weight of the drivetrain, its volume and cost which will meet the propulsion design constraints with minimum power. LEV propulsion system design is to be addressed first.

2.3. Road Load Characteristics

The road load consists of rolling resistance, aerodynamic drag, and climbing resistance. The design of the electric force model incorporates the following force equations:

Rolling Resistance Force,

$$F_f = C_{rr} m_{veh} g \# \tag{1}$$

where $C_{rr,}$the coefficient of rolling resistance is, m_{veh} is the curb weight (kg) or total mass of the LEV, and$g$ is the gravity (9.8 m s^{-2}). This force is due to the friction of the scooter tire on the road, which can be determined depending on rolling resistance and scooter weight.

Aerodynamic Drag Force,

$$F_d = 0.5 C_d A_f \mathrm{p}_a v_{eff}^2 \# \tag{2}$$

Where C_d is the drag coefficient, A_f is the front area (m^2), p density of the air (kg m^{2-}), and $v_{eff} = v_{veh} + v_{air}$, is velocity of the vehicle relative to air.

This force is determined by the scooter's body design and the airborne surface area.

Hill Climbing Force,

$$F_h = F_g sin(\alpha) = m_{veh} g sin(\alpha) \# \tag{3}$$

This force is related to the acting slope and vehicle weight, whereF_g is the gravitational force and α is the slope.

Inertial Force,

$$F_i = m_{veh} a \# \tag{4}$$

where a is the acceleration. This force is the linear acceleration of the scooter, derived from Newton's second law.

Total Propulsion Force is the sum of all the above forces, given by,

$$F_p = F_f + F_d + F_h + F_i \# \tag{5}$$

Components of these forces acting on the vehicle are shown in **Figure 5**. The Total Propulsion Force will decide the vehicle's acceleration and deceleration. Hence, there should be an effort to overcome these forces by delivering the desired power through the propulsion system of the vehicle to the ground/road via the wheels and tires of the vehicle. The choice of motor must overcome the forces in order to move the scooter in forward direction.

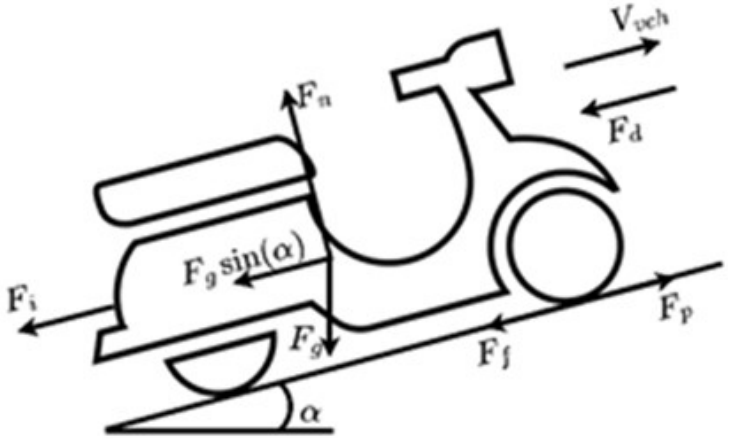

Figure 5. Longitudinal free body diagram of the forces acting on LEV.

The force model of the system will be:

$$F_P = m_{veh}\frac{dV_{veh}}{dt} + F_d + F_f + F_g \sin(\alpha) \# \tag{6}$$

The required tractive power applied by the motor is calculated as below:

$$P_P = F_P V_{veh} = m_{veh}\frac{dV_{veh}}{dt}V_{veh} + F_d V_{veh} + F_f V_{veh} + F_g \sin(\alpha)\, V_{veh} \# \tag{7}$$

$$P_P = m_{veh}\frac{dV_{veh}}{dt}V_{veh} + P_d + P_f + P_g \# \tag{8}$$

Where P_d is the "drag power", applied to the vehicle because of aerodynamic friction, which is described by Equation (9), P_f is the frictional power between the road and the wheels, which is shown in Equation (10), and P_g is the power exerted by gravitation and is described in Equation (11). Drag power is given by the equation

$$P_d = F_d V_{veh} = \frac{1}{2} C_d A_f p_a v_{eff}^2 V_{veh} \# \tag{9}$$

Frictional power is given by the equation

$$P_f = F_f V_{veh} = C_{rr} F_n V_{veh} \# \tag{10}$$

Here C_{rr}= Coefficient of rolling resistance and is given by,

$$C_{rr} = 0.01\left(1 + \frac{3.6}{100} V_{veh}\right)$$

F_n = Normal force = $m_{veh}g$, and g is the acceleration due to gravity.
Gravitational power is given by the equation

$$P_g = F_g \sin(\alpha)\, v_{veh} = m_{veh} g \sin(\alpha)\, v_{veh} \# \tag{11}$$

Power available at the wheels of the LEV without gear ratio is expressed as below:

$$P_M = T_{em}\frac{V}{R_{wheels}} \# \tag{12}$$

Here T_{em}= Electromagnetic torque of the motor (N.m), V = Speed of vehicle (m s^{-1}), R_{wheels} = Wheel radius (m).

Vehicle speed is corresponding to the motor speed and is given by

$$V = \omega_m \times 0.47d = \frac{2\pi \times 0.47d \times n_m}{60} \# \tag{13}$$

Where ω_m= angular velocity of the wheel (1 s^{-1}), d= wheel outer diameter (m), n_m= rotational speed of the wheel (min^{-1}).

The LEV in this design is without transmission, and the motor of the LEV is directly fixed to the wheel. Therefore, the transmission ratio is =1, and propulsion efficiency [η] is = 100%. Therefore, the power available at the wheels $P_M = P_P$ tractive power applied by the motor or the motor effective power.

Torque on the wheels $T_M = T_{em}$ Electromagnetic torque of the motor (N-m) and is given by:

$$T_M = T_{em} = \left(F_f + F_d + F_n + F_i\right) 0.47d\# \quad (14)$$

Therefore, for the appropriate choice of motor specification suitable for the LEV, the force model, tractive power to be applied by the motor and the torque on the wheels are to be determined. For this case study, the chosen vehicle parameters are given in **Table 3**.

Table 3. Vehicle parameters.

Sl.No.	Parameters	Value
1.	Curb weight (kg) or mass of the LEV	200 kg
2.	Front area	0.6 m^2
3.	Velocity of the vehicle	50 km h^{-1}
4.	Density of the air at 20 °C	1.204 kg m^{-3}
5.	Coefficient of rolling resistance	0.015
6.	Drag coefficient	0.7
7.	Tire diameter	416 mm
8.	Density of air at 20 °C	1.2041 kg m^{-3}
9.	Speed	42 km h^{-1}
10.	Capacity of gradient @ 10%	30 km h^{-1}
11.	Capacity of gradient @ 20%	20 km h^{-1}
12.	Maximum acceleration	0.65 m s^{-2}
13.	Maximum deceleration	−0.63 m s^{-2}
14.	Battery voltage	48 V
15.	Time for 1 cycle	108 s

A typical road load (Fr) characteristic as a function of vehicle speed is shown in **Figure 6**.

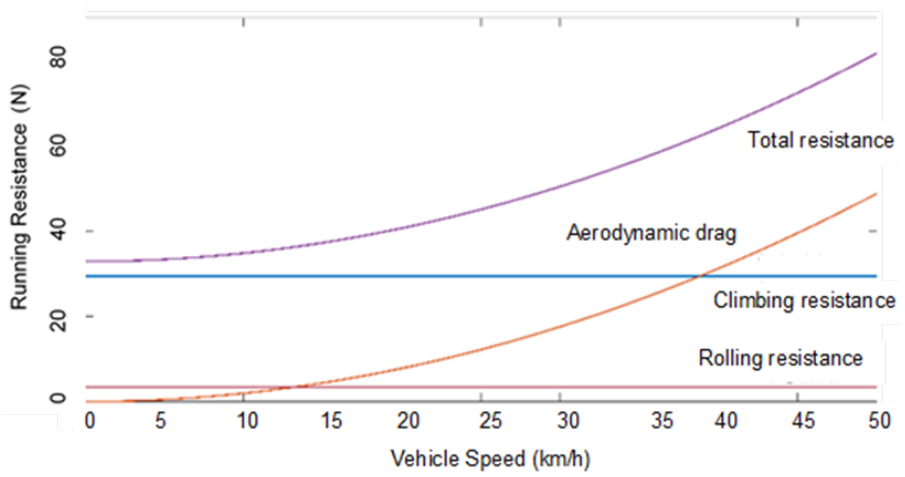

Figure 6. Typical road load characteristics as a function of vehicle speed.

The vehicle parameters of **Table 3** are considered with the following assumptions [22]:

Rolling resistance is independent of velocity; Headwind velocity is zero; Level ground surface.

The total propulsion force, F_p available from the propulsion system is partly consumed in overcoming the road load, and the remaining total propulsion force, F_p accelerates or decelerates the vehicle when road load exceeds F_p.

Therefore, acceleration

$$a = \frac{dv}{dt} = \frac{F_p - F_r}{m_{veh}} \# \tag{15}$$

The boundary conditions are:
at $t = 0, velocity\ of\ the\ LEV\ = 0$
at $t = t_s, velocity\ of\ the\ LEV\ = v_{rv}$

For the rated motor power, P_m, the closed-form solution is obtained by solving Equation (15) by further simplifying the assumptions as: Rolling resistance = 0, aerodynamic drag = 0, and level ground surface. This closed-form solution is suitable for the more practical design involving running resistances.

Closed-form solution for rated motor power

$$P_m = m\int_0^{v_{rv}} \frac{dv}{F_p} = \int_0^{t_s} dt \# \tag{16}$$

Solving Equation (16),

$$P_m = \frac{m}{2t_s}\left({v_{rm}}^2 + {v_{rv}}^2\right) \# \tag{17}$$

The above Equation (17) is obtained by considering the integral as two parts:
$Constant\ force\ operation\ = 0 - v_{rm}$ and
$Constant\ power\ operation\ = 0 - v_{rv}$

Motor minimum power is obtained by differentiating P_m with respect to m and equating to zero. Therefore,

$$v_{rm} = 0 \# \tag{18}$$

When v_{rm} = 0, the motor operates in the constant power region. Therefore, if the motor operates $0 - v_{rv}$ int_s seconds only in constant power region, then the required power is minimum. On the other hand, if the motor operates in the constant force/torque region for the period, $0 - t_s$ then v_{rm}= v_{rv}. As a result, the required power is twice that of the constant power region from Equation (17). The power requirements of the motor between these two boundaries are shown as a solid line in **Figure 7**.

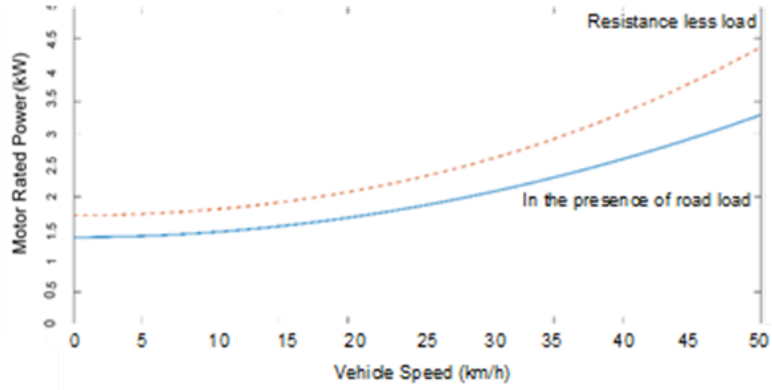

Figure 7. Acceleration power requirement as a function of motor rated speed; continuous curve—without resistance/resistance less, and dashed curve—in the presence of running resistance/road load.

Now, by considering the running resistance, F_r, the closed-form solution will be a transcendental equation for the similar boundaries of Equation (15). This transcendental equation is solved numerically for P_m for specific rated motor speed, v_{rm}, by using the secant method or any other standard root-seeking method [23]. As a result, the rated motor power, P_m, for the vehicle parameters of **Table 3**, and for the assumptions (1) headwind velocity is zero (2) level ground surface is as shown in **Figure 7** as a dotted line.

From the dotted line of **Figure 7**, the following conclusions are made. Rated motor power, P_m vs. rated motor speed v_{rm} is of similar nature as in the case when running resistance, $F_r = 0$.

Rated motor power, P_m is minimum for continuous constant power operation v_{rm} = 0.

Rated motor power, P_m is approximately twice that of the constant power operation for the continuous constant force/operation $v_{rm} = v_{rv}$.

Rated motor power, $P_m =$ 1.3 kW as shown from **Figure 7** remains approximately minimum up to about 10 km h^{-1} of rated speed and then increases rapidly.

Case Study—Force Model:

The force model is needed to assess the power required to accelerate and run the vehicle at desired speeds. **Figure 8** shows the force-speed characteristics for the vehicle parameters of **Table 3**. The force required is dependent on the gradient. For the gradients at 0%, 10%, 20%, and 30%, the determined force is 78.28 N, 243.18 N, 429.66 N, and 620 N respectively. The force profile is obtained by connecting the points from P_0 to P_3 of the graph as shown, and in addition to this, by adding a safety margin; the effective force can be estimated. The power-speed characteristics for different dynamic road conditions are as shown in **Figure 9**, in which for 0% gradient at 35 km h^{-1} and at 50 km h^{-1} the power is 0.518 kW and 1.08 kW respectively. This design procedure of EPS based on vehicle dynamics is useful to arrive at the required motor power rating.

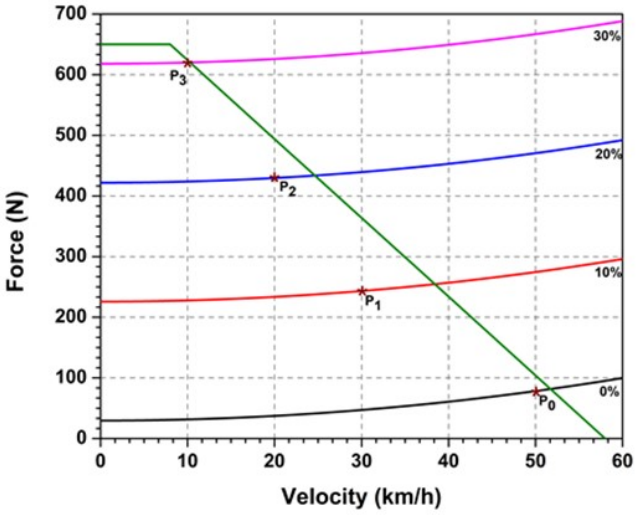

Figure 8. EPS force-speed characteristics.

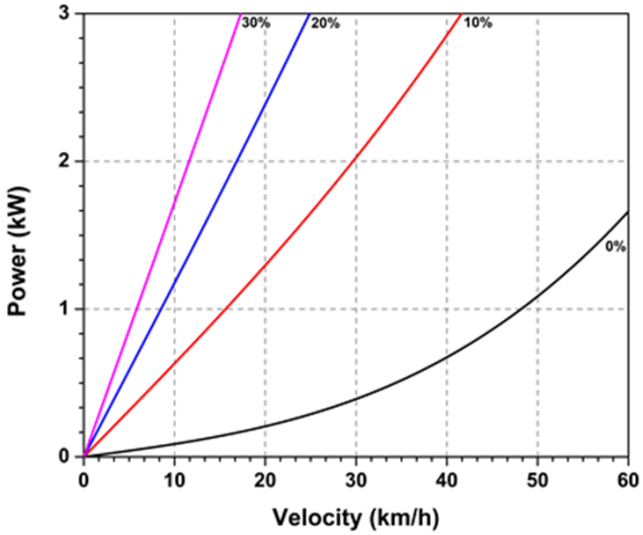

Figure 9. EPS power-speed characteristics.

The maximum speed at which the LEV climbs the ramp for $\alpha_{max} = 15^{\circ}$ is $V_{ramp} = 10$ km h^{-1} and for if $\alpha_{max} = 20^{\circ}$ =7.7 km h^{-1}.

Analytically, this value is obtained by Equation (19).

$$V_{ramp} = \frac{1000\eta_{tr}P_{max}}{mg(f cos\alpha_{max} + sin\alpha_{max})}\# \quad (19)$$

Where η_{tr}= transmission coefficient = 1.

3. Drive Cycle Analysis to Choose Power Rating of Motor

The driving cycle is utilized as a standard tool for the evaluation of vehicle characteristics, energy consumption economy, electric vehicle autonomy, polluting emissions, and driving range in the automobile industry. The estimation of vehicle parameters depends on the driving cycle used. The chosen driving cycle determines the power required for the particular vehicle parameters. The time profile of velocity (V) explains the driving characteristics of a given vehicle in real-time driving conditions. It consists of (1) speed components and (2) road gradient components, but normally one of the components is kept constant while the other is varied. The procedure for developing the driving cycle mainly consists of four steps: namely, roadway, compilation of statistics, driving cycle and assessment, in order to provide information on the on-road driving environment [24–26]. **Figure 10** shows the general procedural steps for the driving cycle.

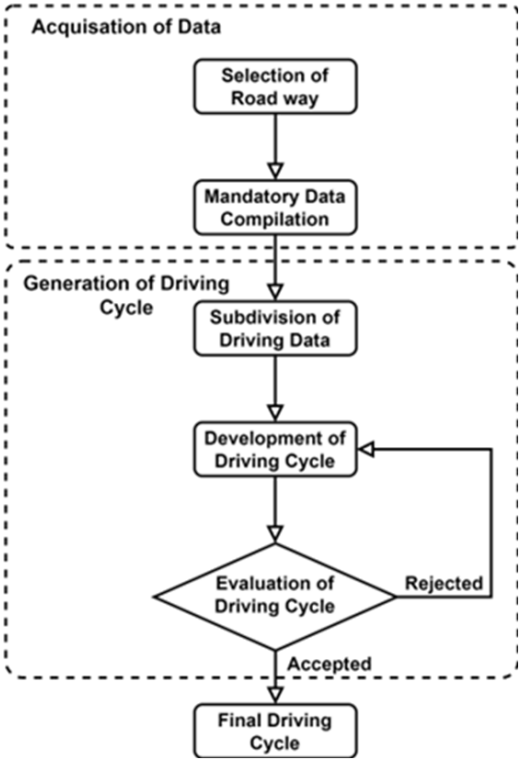

Figure 10. General procedure for driving cycle.

3.1. Case Study

Vehicle parameters from **Table 3** above are used to develop the powertrain model. For the evaluation of driving, two driving cycles namely the New European Driving Cycle (NEDC) and the Indian Driving Cycle (IDC), have been considered.

The NEDC has a maximum speed of 120 km h^{-1}, an average speed of 33.2 km h^{-1}, a duration of 1184 s, and a length of 10.9 km [27]. The NEDC profile is shown in **Figure 11**. Depending on the repetition of the driving cycle, the desired acceptable distance can be calculated. The IDC has a maximum speed of 42 km h^{-1}, an average speed

of 21.93 km h^{-1}, a duration of 108 s, and a length of 0.65 km. The IDC profile is shown in **Figure 12a**.

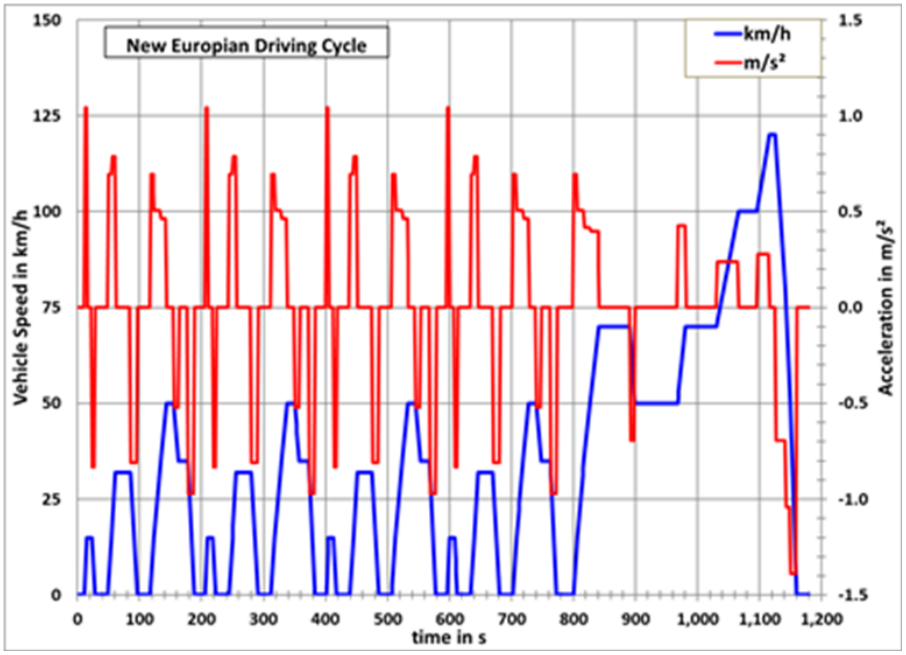

Figure 11. New European Driving Cycle (NEDC) profile.

For Indian road conditions, the IDC is considered. This IDC profile is developed by the Automotive Research Association of India (ARAI) as per IS 15886:2010 [28]. For the IDC profile, with a duration of 1188 seconds at an average speed of 21.93 km h^{-1}, the distance travelled is 7.238 km with a repetition of 11 driving cycles, as shown in **Figure 12b**.

In general, the satisfying needs of the standard two-wheeler driver are (1) a driving range of approximately 120 km, (2) good acceleration (around 6 seconds from 0 to 50–60 km s^{-1}), and (3) a peak speed of approximately 70–75 km h^{-1}. The energy storage system (ESS) is one of the key components of LEV, in which batteries are the most widely used. However, the shortfall of battery-based ESS is reduced battery lifespan, with low power density; hence, the driving range is limited. The Indian city driving condition has a lower driving speed with a greater number of stops and a high level of maximum acceleration and deceleration. As a result, there will be a greater number of stop-and-depart conditions, which may produce a considerable level of fuel savings with LEV.

The vehicle speed corresponds to the motor speed, and both motor speed and motor torque are dependent on the vehicle parameters and motion conditions. The motion conditions are defined by the vehicle velocity and at the same time, the resistance to motion determines the instant motor load [26, 29]. Therefore, both the vehicle parameters and driving cycle data are necessary to calculate the torque. From **Table 3** and from the above Equations (13) and (14) the velocities and torque can be calculated. **Figure 13** shows the torque profile for both NEDC and IDC. From the NEDC profile in **Figure 11**, corresponding to the maximum acceleration of 1.04 m sec^{-2} at 14 s, the torque developed is 46.96 N-m which can be observed from the torque profile in **Figure 13**. From the IDC profile of **Figure 12a** corresponding to the maximum acceleration of 0.65 m sec^{-2} at 20 s, the torque developed is 31.61 N-m as seen from the torque profile in **Figure 13**. For a 0° inclination, the velocities at 10, 20, 30 and 50 km h^{-1} yield determined torques of 6.13, 7.28, 9.19, and 15.29 N-m respectively. Similarly, for different inclinations and velocities, torque can also be calculated. Hence, from the developed force model in **Figures 8** and **9** and from the torque profile in **Figure 13**, it is observed that both the analytical and simulation results of force and torque parameters are in agreement. For a 0° inclination, the torque at 50 km h^{-1} is 15.29 N-m and the corresponding force is 72.18 N. From **Figure 14**, the determined maximum power to be supplied by the motor for the IDC profile at 66 s is 0.67 kW and for the NEDC profile at 1184 s is 5.617 kW. Hence, from the NEDC power profile, it is observed that for a speed of 120 km h^{-1}, the power required is 5.617 kW. From the IDC profile it is observed that, for a speed of 42 km h^{-1} power required is 0.67 kW.

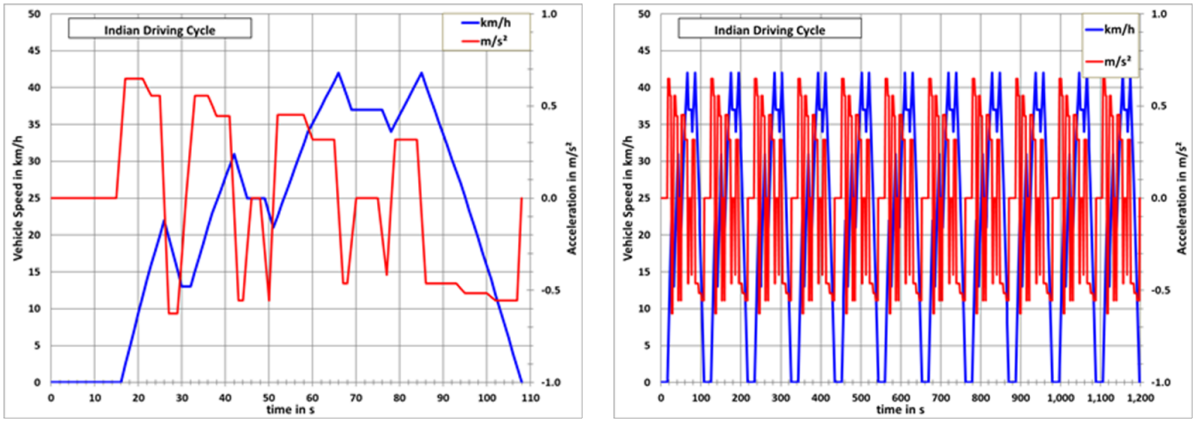

(**a**) (**b**)

Figure 12. (**a**) Indian Driving Cycle (IDC) profile, and (**b**) IDC profile for 1188 seconds.

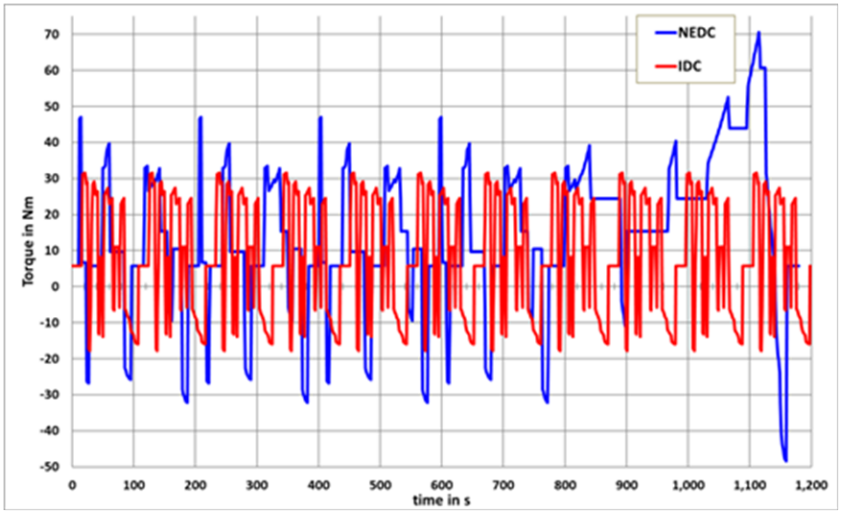

Figure 13. Torque profile – NEDC and IDC.

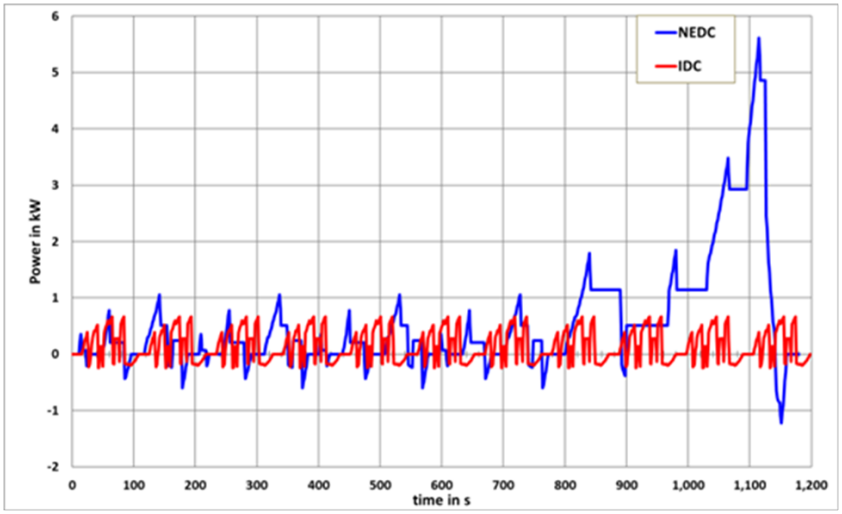

Figure 14. Power profile – NEDC and IDC.

In this design and analysis, the chosen motor is directly placed inside the wheel without transmission or gears. The main advantages of such type of EPS are reduced weight, enhanced efficiency, improved aerodynamics, and additional driving capabilities like spot turning and side driving. Therefore, for Indian road conditions and for the chosen vehicle parameters in **Table 3**, such as weight, volume, IDC, transport operating and temperature conditions, safety, reliability, and cost economics, EPS with an in-wheel motor is preferred. Hence, for the above vehicle parameters and IDC data, and in addition to a safety margin factor at 25%, including market standards, it is preferred to opt for a 1.5 kW PMBLDC hub motor.

The objective of this simulation case study is to confirm the power rating and the procedure to initiate the sizing of the motor. The procedure for sizing the motor depends on drive duty cycle calculation, which is based on motor or vehicle speed. The tire height and the wheel diameter are used to calculate the motor speed. The optimized geometry dimension of the PMBLDC motor can be designed for both outer rotor and inner rotor configurations.

4. Performance Analysis of the LEV Drive

In order to investigate the torque performance, the PMBLDC motor with balanced three-phase, star-connected, symmetrical windings is chosen. **Table 4** shows the parameters chosen for simulation case studies, which are in line with the requirements of vehicle parameters in **Table 3.** The details of the switching sequence, rotor position, position sensor signals, and phase currents are shown in **Table 5**. The PMBLDC motor circuit produces maximum torque when two phases are energized or in the "on" position, while the third phase will be in the "off" position. Depending on the rotor position the phases will be energized. A voltage-fed six-step inverter with similar MOSFET switches is applied to achieve current commutation. The position sensor signals, ideal back EMF, current, and output torque waveforms are shown in **Figure 15**.

Table 4. Parameters chosen for case study.

Parameters	Particulars
Rated voltage, V	48 Volts (DC)
Rated power	1.5 kW
Rated torque	24 N-m
Rated speed, N	1000 RPM
Stator resistance, R_a	0.2 Ω
Stator self inductance, L_a	1 mH
Mutual inductances, M	0.2 mH
Back E.M.F per phase, e	42 V
Per phase current, i_{rms}	46.68 A
Back EMF	Trapezoidal
Back EMF constant, K_e	1.684 V rad^{-1} s^{-1}
Torque developed by the motor, T_e (@ no-load)	24 N-m
Maximum power	1.8 kW
Maximum torque	48.9 N-m
Maximum current	160.1 A
Torque constant, k_t	1.684 N-m A^{-1}
Moment of Inertia, J	0.00512 kg-m^2

Table 5. Inverter switching sequences details.

Switching Sequence	Rotor Position, θ_e (deg)	Hall Sensor			PWM Switching (Active Switches)		Phase Currents		
		H1	H1	H2			A	B	C
1	0–60°	1	1	0	S5	S4	Off	−	+
		1	1	0	S1	S4	+	−	Off
2	60–120°	0	1	0	S1	S4	+	−	Off
		0	1	0	S1	S6	+	Off	−

Table 5. *Cont.*

Switching Sequence	Rotor Position, θ_e (deg)	Hall Sensor			PWM Switching (Active Switches)		Phase Currents		
		H1	H1	H2			A	B	C
3	120–180°	0	1	1	S1	S6	+	Off	−
		0	1	1	S3	S6	Off	+	−
4	180–240°	0	0	1	S3	S6	Off	+	−
		0	0	1	S3	S2	−	+	Off
5	240–300°	1	0	1	S3	S2	−	+	Off
		1	0	1	S5	S2	−	Off	+
6	300–360°	1	0	0	S5	S2	−	Off	+
		1	0	0	S6	S4	Off	−	+

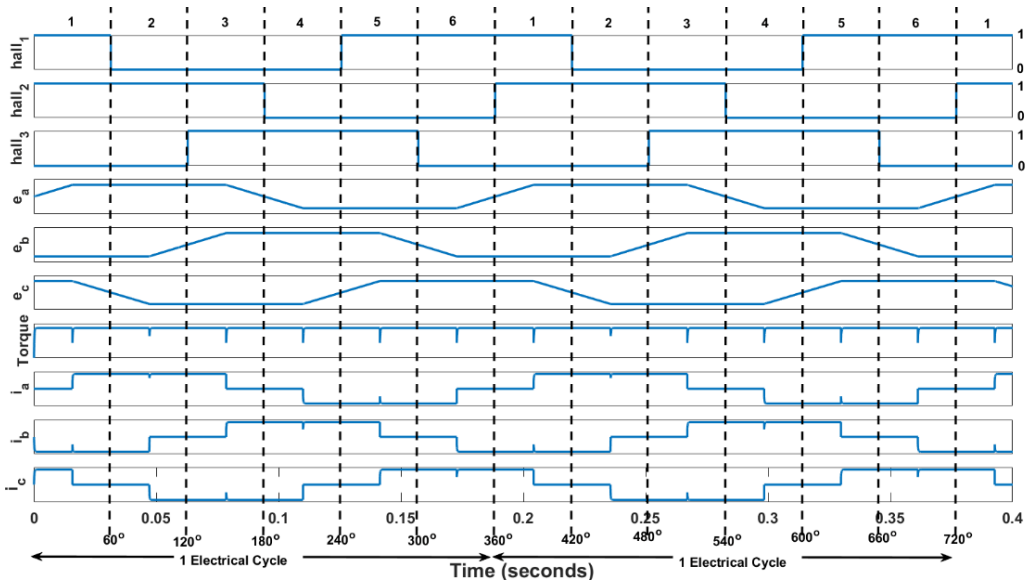

Figure 15. Waveforms: position sensor signals, ideal back EMFs, torques, and current waveforms.

The PMBLDC motor transfer function at the no-load condition is given in Equation (20) and the transfer function of the PID controller in generic form is given in Equation (21)

$$G_u(s) = \frac{\omega(s)}{V_s(s)} = \frac{K_t}{JL_a s^2 + (JR_a + BL_a)s + (BR_a + K_t K_e)} \tag{20}$$

$$G_c(s) = K_p + \frac{K_i}{s} + K_d s \tag{21}$$

Where K is the gain of the controller, which increases the response speed of the controller.

The closed-loop transfer function of the drive is given in Equation (22):

$$G_{cl}(s) = \frac{G_u(s)\,G_c(s)}{1 + G_u(s)\,G_c(s)} \tag{22}$$

By substituting the values of PMBLDC motor parameters from **Table 5** along with $k_t = 1/k_v, k_e = k_t$, $k_f = 0$, $B = 0$ and the values of K_P and K_I parameters, which are fine-tuned using MATLAB's PID tuner block, the system is set for stable operation with high-speed response. The obtained values are $K_p = 0.05$ and $K_i = 50$. This proposed PI speed controller data is chosen for performance analysis of the proposed LEV drive. The effect of K_p and K_i on step response is shown in **Figure 16**.

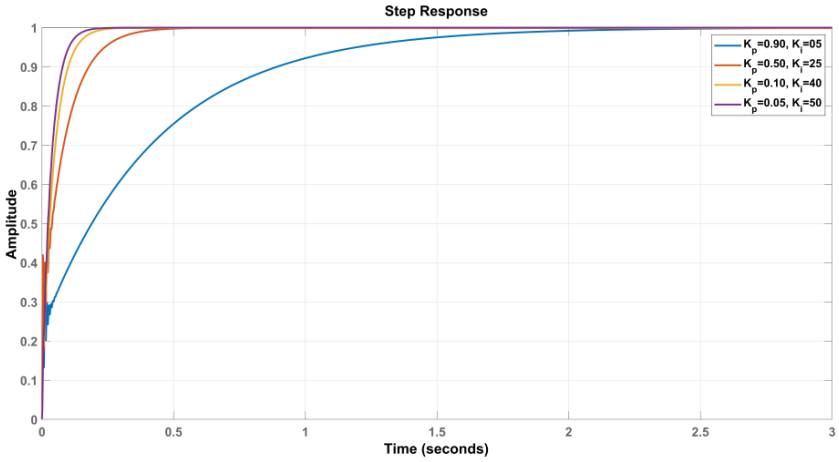

Figure 16. Effect K_p of and K_i on step response.

Performance analysis of the PMBLDC hub motor-based LEV drive at rated speed and under different drive conditions has been evaluated from the performance characteristics, as shown in **Figure 17**. These characteristics include output power, output torque, efficiency and input DC current. It is observed that the distortions in the input current can be eliminated by the controller; as a result, smooth motor torque will be generated. The efficiency for the proposed motor across the full speed range has been obtained. It is observed from the simulation studies that the efficiency is high, at about 90% for about 1430 rpm, and the maximum output power is about 48.52 kW at 715 rpm, reaching zero at 1500 rpm.

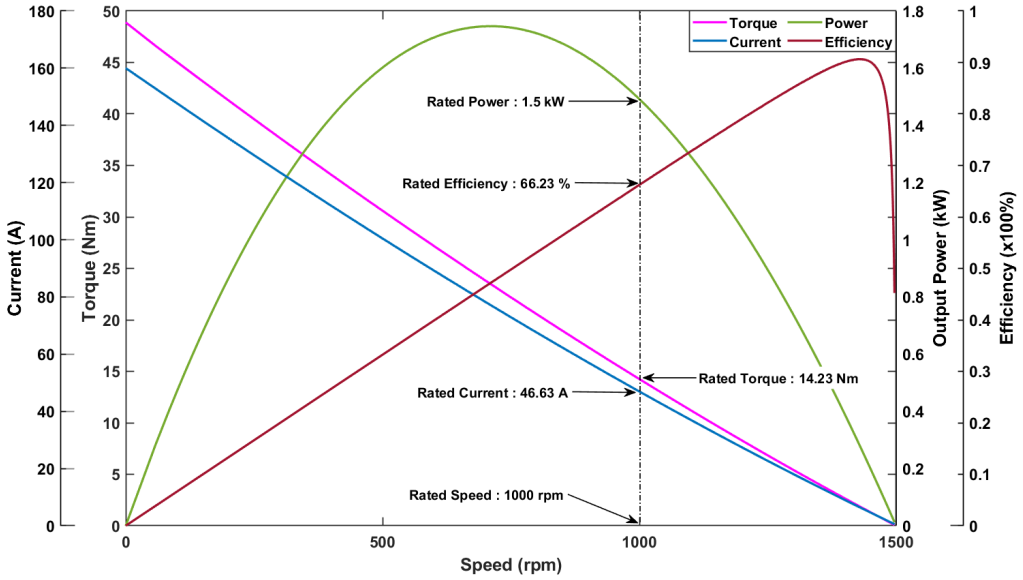

Figure 17. Simulated performance characteristics of the chosen BLDC motor, namely power, torque, efficiency, and current at different LEV drive conditions.

Also, the starting high input motor current yields a considerable magnetic saturation level of the stator during which the motor speed is much lower, and as this motor speed increases, the input motor current starts decreasing and reaches zero at 1500 rpm. The motor rated torque generated is 14.23 N-m without saturation. Hence, it is found from the performance analysis of the drive that the chosen PMBLDC motor with a 1.5 kW rating is capable of overcoming all the force parameters such as aerodynamic drag, rolling resistance drag and kinetic resistance,

thereby propelling the electric scooter smoothly in the forward direction.

5. EPS Experimental Implementation

The experimental setup as shown in **Figure 18**, mainly consists of (1) a 48 V battery pack supplying power under varying load conditions as the energy source, (2) an H-bridge, (3) a microcontroller GPM8F3108A used as a motor controller optimized for real-time control, (4) the driver circuit: an IR2130 pre-driver chip with bootstrap functionality to manage motor phase currents, and (5) oscilloscopes and data loggers as measurement tools used to record voltage, current, and torque profiles. The experimental results under varying conditions as as follows: (1) motor speed of 250 RPM with reduced acceleration, and speed of 2000 RPM with full acceleration both for without load conditions, as shown in **Figure 19a,b**, and (2) the motor applied voltage and phase current for 1300 RPM without load and 750 RPM with load conditions, as shown in **Figure 20a,b**, respectively. The experimental results were consistent with simulation predictions, as per the data comparision in **Table 6**, confirming the robustness and reliability of the propulsion system design.

Ripple in the output torque can be validated through the current waveform and it is clearly visible in **Figure 19** that the ripple in current is minimal. On the experimental scale, for an output current in the range of 20 A, ripple content is restricted to 317 mA, which indicates very minimal torque pulsation, as shown in **Figure 19b** below. A similar analysis can be considered for other figures. Torque pulsation is significant at higher speeds and reduces with an increase in speed.

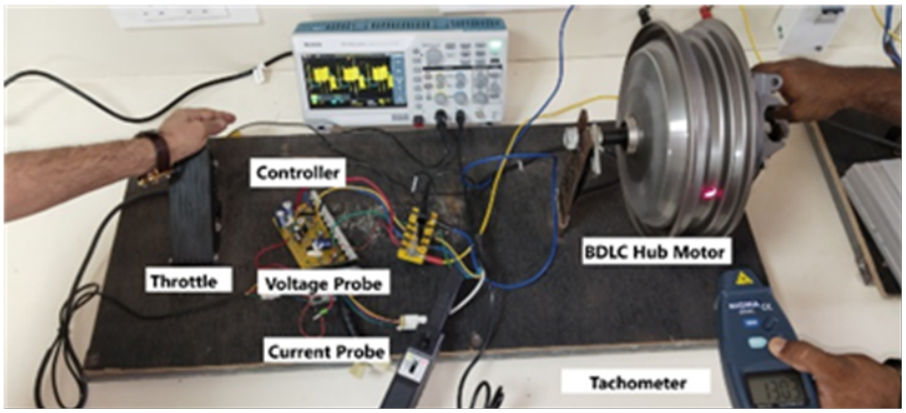

Figure 18. Experimental setup for PMBLDC hub motor drive.

(**a**)

Figure 19. *Cont.*

(**b**)

Figure 19. Motor speed without load, (**a**) at 250 RPM and with reduced throttle, and (**b**) at 2000 RPM and with full throttle.

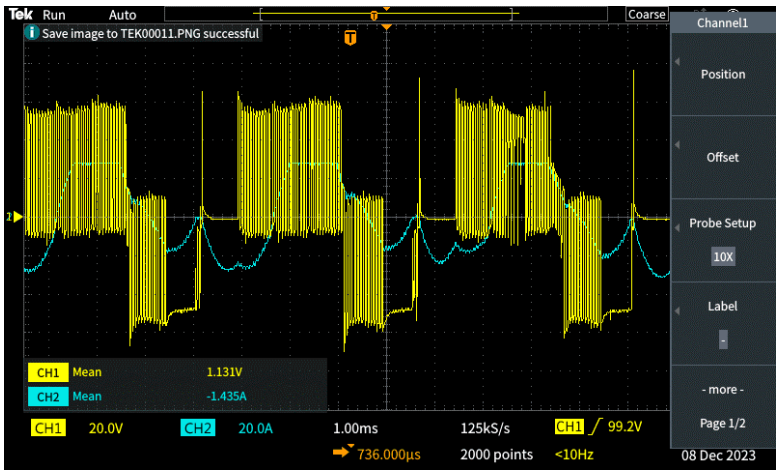

(**a**)

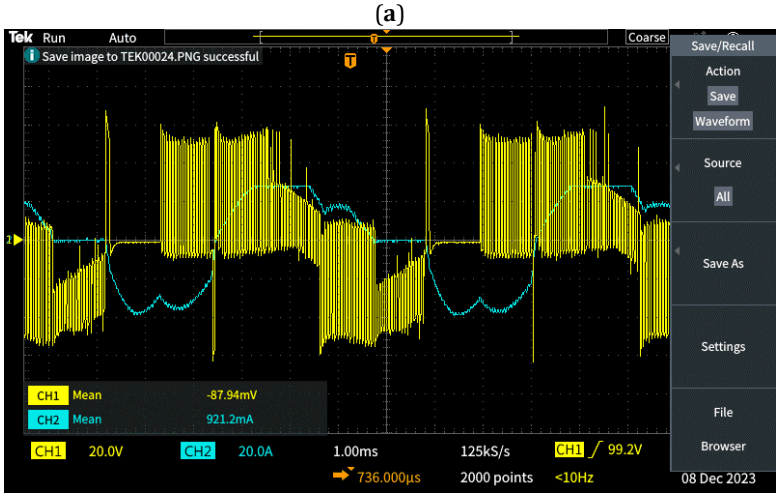

(**b**)

Figure 20. Line voltage and phase current (**a**) for 1300 RPM without load, and (**b**) for 750 RPM with load.

Table 6. Result comparison of parameters.

Parameters	Simulation Result	Experimental Result	Percentage Error
Efficiency (%)	90.0	88.5	1.67%
Torque (Nm)	14.23	14.10	0.91%
Output power (kW)	1.75	1.7	2.85%

6. Conclusions

This paper presents the LEV propulsion system design philosophies based on vehicle dynamics, addressing gaps in existing research by integrating vehicle dynamics, driving cycle analysis, and motor power optimization. The study demonstrates the advantages of employing a 1.5 kW PMBLDC motor for LEV applications, particularly in urban and semi-urban environments. This methodology of study and analysis of propulsion system design aims to find the best possible torque-speed profile for the LEV propulsion system and to overcome vehicle operational constraints with minimum power requirements. Additionally, the study reveals that wide-range constant power region operation beyond the rated speed is vital for both (1) the initial acceleration interval, and (2) cruising intervals of operation. The two critical factors (1) performance and (2) efficiency required for LEV have been achieved through both high torque density and low torque ripple. These two key findings include the critical role of operating in the constant power region and the benefits of a gearless in-wheel motor design. Design optimization and PI control strategies of the drive have reduced torque ripple. A higher torque density means a motor can deliver more torque for its size, which is crucial for compact and efficient LEVs.

In addition, the power requirement for acceleration will be minimal if the motor operates more in the constant power region. Based on the study of several types of motors, it is concluded that the PMBLDC hub motor is the best suitable choice at present. However, detailed design and evaluation have to be verified. These propulsion system design philosophies are applied to LEV to demonstrate their advantages and viabilitiy. This methodology of design will serve only as a foundation to develop a detailed LEV drive, which is a more intricate process.

By minimizing power consumption and ensuring robust performance across varying conditions, the proposed methodology provides a foundation for cost-effective and efficient LEV propulsion systems. Future work will focus on extending the methodology to larger EVs, exploring advanced control algorithms such as AI-based systems for real-time torque-speed optimization and integrating next-generation batteries, such as solid-state or lithium-sulfur technologies, to enhance driving range.

Author Contributions

Conceptualization, methodology, software, investigation, writing—original draft preparation, S.S.; visualization, editing draft, review, supervision, S.R. All authors have read and agreed to the published version of the manuscript.

Funding

This work received no external funding.

Institutional Review Board Statement

Not applicable.

Informed Consent Statement

Not applicable.

Data Availability Statement

No new data were created in this work.

Conflicts of Interest

The authors declare no conflict of interest.

References

1. AR6 Synthesis Report: Climate Change 2023. IPCC Report 2023 . Available from: https://www.ipcc.ch/report/ar6/syr/ (accessed on 4 April 2025).
2. Chan, C.C. The State of the Art of Electric and Hybrid Vehicles. *Proc. IEEE* **2002**, *90*, 247–275. [CrossRef]
3. Kumar, L.; Jain, S. Electric Propulsion System for Electric Vehicular Technology: A Review. *Renew. Sustain. Energy Rev.* **2014**, *29*, 924–940. [CrossRef]
4. Bertoluzzo M.; Buja, G. Development of Electric Propulsion Systems for Light Electric Vehicles. *IEEE Trans. Ind. Inform.* **2011**, *7*, 428–435. [CrossRef]
5. Emadi, A. Transportation 2.0. *IEEE Power Energy Mag.* **2011**, *9*, 18–29. [CrossRef]
6. Zhu, Z.Q.; Howe, D. Electrical Machines and Drives for Electric, Hybrid, and Fuel Cell Vehicles. *Proc. IEEE* **2007**, *95*, 746–765. [CrossRef]
7. Barroso, D.G.; Yang, Y.; Machado, F.A.; et al. Electrified Automotive Propulsion Systems: State-of-the-Art Review. *IEEE Trans. Transp. Electrif.* **2022**, *8*, 2898–2914. [CrossRef]
8. GmbH, R.B. *Bosch Automotive Handbook*, 7th ed.; Robet Bosch GmbH: Plochingen, Germany & Bentley Publishers: Cambridge, MA, USA, 2007.
9. Hsin-Chang, C.; Rohman, Y.F.; Ashlah, M.B.; et al. Electrification of Agricultural Machinery: One Design Case of a 4 kW Air Compressor. *Energies* **2024**, *17*, 3647. [CrossRef]
10. Shao, L.; Navaratne, R.; Popescu, M.; et al. Design and Construction of Axial-Flux Permanent Magnet Motors for Electric Propulsion Applications—A Review. *IEEE Access* **2021**, *9*, 158998–159017. [CrossRef]
11. Pellegrino, G.; Vagati, A.; Boazzo, B.; et al. Comparison of Induction and PM Synchronous Motor Drives for EV Application Including Design Examples. *IEEE Trans. Ind. Appl.* **2012**, *8*, 2322–2332. [CrossRef]
12. Yang, Z.; Shang, F.; Brown, I.P.; et al. Comparative Study of Interior Permanent Magnet, Induction, and Switched Reluctance Motor Drives for EV and HEV Applications. *IEEE Trans. Transp. Electrif.* **2015**, *1*, 245–254. [CrossRef]
13. Hashemnia N.; Asaei, B. Comparative Study of Using Different Electric Motors in the Electric Vehicles. In Proceedings of the 2008 International Conference on Electrical Machines, Vilamoura, Portugal, 9 September 2008. [CrossRef]
14. Abdelhafez, A.A.; Aldalbehi, M.A.; Aldalbehi, N.F.; et al. Comparative Study for Machine Candidates for High Speed Traction Applications. *Int. J. Electr. Eng.* **2017**, *10*, 71–84.
15. Wang, J.; Zhang, C.; Guo, D.; et al. Drive-Cycle-Based Configuration Design and Energy Efficiency Analysis of Dual-Motor 4WD System With Two-Speed Transmission for Electric Vehicles. *IEEE Trans. Transp. Electrif.* **2024**, *10*, 1887–1899. [CrossRef]
16. Bertoluzzo, M.; Buja, G.; Keshri, R.K.; et al. Analytical Study of Torque vs. Speed Characteristics of PM Brushless DC Drives. In Proceedings of the IECON 2012 - 38th Annual Conference on IEEE Industrial Electronics Society, Montreal, QC, Canada, 25–28 October 2012. [CrossRef]
17. Gan, J.; Chau, K.T.; Chan, C.C.; et al. A New Surface-Inset, Permanent-Magnet, Brushless DC Motor Drive for Electric Vehicles. *IEEE Trans. Magn.* **2000**, *36*, 3810–3818. [CrossRef]
18. Bhatt, P.; Mehar, H.; Sahajwani, M. Electrical Motors for Electric Vehicle – A Comparative Study. In Proceedings of the Recent Advances in Interdisciplinary Trends in Engineering & Applications (RAITEA), Indore, India, 16 February 2019. [CrossRef]
19. Kumar M.S.; Revankar, S.T. Development Scheme and Key Technology of an Electric Vehicle: An Overview. *Renew. Sustain. Energy Rev.* **2017**, *70*, 1266–1285. [CrossRef]
20. Ravi, N.; Ekram, S.; Mahajan, D. Design and Development of a In-Wheel Brushless D.C. Motor Drive for an Electric Scooter. In Proceedings of the 2006 International Conference on Power Electronic, Drives and Energy Systems, New Delhi, India, 12–15 December 2006. [CrossRef]
21. Bilaţiu, C.-A.; Cosman, S.I.; Marţiş, R.-A.; et al. Identification and Evaluation of Electric and Hybrid Vehicles Propulsion Systems. In Proceedings of the 2019 Electric Vehicles International Conference (EV), Bucharest, Romania, 3–4 October 2019, [CrossRef]
22. Ehsani, M.; Rahman, K.M.; Toliyat, H.A. Propulsion System Design of Electric and Hybrid Vehicles. *IEEE Trans. Ind. Electron.* **1997**, *44*, 19–27. [CrossRef]
23. Ralston, A.; Rabinowitz, P.A. *First Course in Numerical Analysis*; Dover Publications: New York, NY, USA, 2001.

24. Duan, X.; Schockenhoff, F.; Koch, A. Implementation of Driving Cycles Based on Driving Style Characteristics of Autonomous Vehicles. *World Electr. Veh. J.* **2022**, *13*, 108. [CrossRef]
25. Du, G.; Cao, W., Hu, S., et al. Design and Assessment of an Electric Vehicle Powertrain Model Based on Real-World Driving and Charging Cycles. *IEEE Trans. Veh. Technol.* **2019**, *68*, 1178–1187. [CrossRef]
26. Sun, Z.; Shi, Z.; Cai, Y.; et al. Driving-Cycle Oriented Design Optimization of a Permanent Magnet Hub Motor Drive System for a Four-Wheel-Drive Electric Vehicle. *IEEE Trans. Transp. Electrif.* **2020**, *6*, 1115–1125. [CrossRef]
27. Chen, L.; Xu, H.; Sun, X. A Novel Strategy of Control Performance Improvement for Six-Phase Permanent Magnet Synchronous Hub Motor Drives of EVs Under New European Driving Cycle. *IEEE Trans. Veh. Technol.* **2021**, *70*, 5628–5637. [CrossRef]
28. Indian Drive Cycles and RDE Program for Effective Emission Norms, Controls and Policies - Review Report. Available online: https://home.iitk.ac.in/~mukesh/Publications/Indian%20Real%20Driving%20Emission%20Reprort%202021.pdf (accessed on 7 February 2025).
29. Abdel-Wahed, A.T.; Ullah, Z.; Abdel-Khalik, A.S.; et al. Drive Cycle-Based Design with the Aid of Data Mining Methods: A Review on Clustering Techniques of Electric Vehicle Motor Design with a Case Study. *IEEE Access* **2023**, *11*, 115775–115797. [CrossRef]